JIPB Journal of Integrative Plant Biology

Research Article
https://doi.org/10.1111/jipb.13542

TaTIP41 and TaTAP46 positively regulate drought tolerance in wheat by inhibiting PP2A activity

Jianhui Ma[1†], Yuke Geng[2,3†], Hong Liu[2†], Mengqi Zhang[1], Shujuan Liu[2], Chenyang Hao[2], Jian Hou[2], Youfu Zhang[2], Daijing Zhang[1], Weijun Zhang[4], Xueyong Zhang[2*] and Tian Li[2*]

1. College of Life Sciences, Henan Normal University, Xinxiang 453007, China
2. Key Laboratory of Crop Gene Resources and Germplasm Enhancement, Institute of Crop Sciences, Chinese Academy of Agricultural Sciences, Beijing 100081, China
3. College of Life and Environmental Science, Minzu University of China, Beijing 100081, China
4. Crop Research Institute, Ningxia Academy of Agriculture and Forestry Sciences, Yinchuan 750002, China

†These authors contributed equally to this work.

*Correspondences: Tian Li (litian@caas.cn, Dr. Li is responsible for the distribution of all materials associated with this article); Xueyong Zhang (zhangxueyong@caas.cn)

Jianhui Ma

Tian Li

ABSTRACT

Drought is a major environmental stress limiting global wheat (*Triticum aestivum*) production. Exploring drought tolerance genes is important for improving drought adaptation in this crop. Here, we cloned and characterized *TaTIP41*, a novel drought tolerance gene in wheat. TaTIP41 is a putative conserved component of target of rapamycin (TOR) signaling, and the *TaTIP41* homoeologs were expressed in response to drought stress and abscisic acid (ABA). The overexpression of *TaTIP41* enhanced drought tolerance and the ABA response, including ABA-induced stomatal closure, while its downregulation using RNA interference (RNAi) had the opposite effect. Furthermore, TaTIP41 physically interacted with TaTAP46, another conserved component of TOR signaling. Like TaTIP41, TaTAP46 positively regulated drought tolerance. Furthermore, TaTIP41 and TaTAP46 interacted with type-2A protein phosphatase (PP2A) catalytic subunits, such as TaPP2A-2, and inhibited their enzymatic activities. Silencing *TaPP2A-2* improved drought tolerance in wheat. Together, our findings provide new insights into the roles of TaTIP41 and TaTAP46 in the drought tolerance and ABA response in wheat, and their potential application in improving wheat environmental adaptability.

Keywords: ABA response, drought tolerance, PP2A, TaTIP41, TaTAP46, TOR signaling, *Triticum aestivum*

Ma, J., Geng, Y., Liu, H., Zhang, M., Liu, S., Hao, C., Hou, J., Zhang, Y., Zhang, D., Zhang, W., et al. (2023). TaTIP41 and TaTAP46 positively regulate drought tolerance in wheat by inhibiting PP2A activity. J. Integr. Plant Biol. **00:** 1–15.

INTRODUCTION

Wheat (*Triticum aestivum*) is one of the most important staple crops for global food security. As wheat is mainly grown in arid and semi-arid areas, drought is a major factor limiting its production—>40% of the world's wheat fields are subject to drought stress (Lan et al., 2022). Moreover, due to global climate change, drought stress is becoming increasingly frequent and more extreme, leading to severe wheat yield losses; therefore, identifying and utilizing potential drought tolerance genes is of great significance in improving the adaptability of this essential crop. Many drought tolerance genes have been characterized in plants through a combination of genetic, biochemical, and physiological approaches. In wheat, drought tolerance genes are widely involved in the regulation of multiple biological processes, including root development, stomatal aperture, and water use efficiency. *TaNAC071-A* was selected as a candidate gene involved in wheat drought tolerance using a genome-wide association study. Further analysis revealed that a 108-bp insertion in the promoter of *TaNAC071-A*, which can be bound and activated by TaMYBL1, enhances its

expression, and the wheat plants overexpressing *TaNAC071-A* or carrying the 108-bp insertion allele showed higher drought tolerance through improved water use efficiency (Mao et al., 2022a). Moreover, a wheat DREB transcription factor gene (*TaDTG6-B*) was identified as a positive regulator of drought tolerance. A 26-bp gain-of-function deletion in the *TaDTG6-B* coding region resulted in its stronger transcriptional activation, protein interactions, DNA binding activity, and ultimately a greater drought tolerance in wheat seedlings (Mei et al., 2022). As a complex quantitative trait, drought tolerance is controlled by numerous genes, and many genetic components and molecular mechanisms involved in wheat drought tolerance have yet to be investigated.

Abscisic acid (ABA) is one of the most important phytohormones involved in environmental stress responses (Nakashima and Yamaguchi-Shinozaki, 2013). The Pyrabactin Resistance 1/PYR1-like/Regulatory Components of ABA Receptors (PYR1/PYL/RCAR) proteins (PYLs), type-2C protein phosphatases (PP2Cs), and SNF1-related protein kinases 2 (SnRK2s) are the core components of ABA signaling (Cutler et al., 2010). The ABA signaling pathway plays a key role in plant drought tolerance by inducing stomatal closure and reducing water loss (Munemasa et al., 2015). In wheat, the overexpression (OE) of *TaPYL1-1B* exhibited enhanced ABA sensitivity and higher drought tolerance. A favorable allele, *TaPYL1-1B*$^{In\text{-}442}$, carrying a MYB recognition site insertion in its promoter, increased drought tolerance in wheat germplasm (Mao et al., 2022b). The ectopic expression of *TaSnRK2.10* also conferred drought tolerance by decreasing water loss (Zhang et al., 2023). Other components such as transcription factors and signaling proteins also participate in linking ABA signals to their responses in plant cells. Despite their importance, very few ABA signaling components have been characterized in regard to their drought tolerance roles in wheat, and the molecular network linking ABA signaling and the drought response remains to be elucidated.

The target of rapamycin (TOR) is a typical Ser/Thr protein kinase belonging to the phosphoinositide 3-kinase-related kinase family and is structurally and functionally conserved among eukaryotes (Dobrenel et al., 2016). Recently, plant TOR signaling has emerged as a central regulatory hub that integrates diverse internal and external cues to regulate growth, development, and stress responses (Dobrenel et al., 2016; Liu and Xiong, 2022). In yeast, one of the major channels for TOR signaling is type 2A phosphatase-associated protein 42 kDa (TAP42) (Huber et al., 2009). The plant ortholog of TAP42, TAP46, is a positive downstream effector of the TOR signaling pathway in *Arabidopsis thaliana* and *Nicotiana tabacum* (Ahn et al., 2011, 2015). Furthermore, the TAP42-interacting protein of 41 kDa (TIP41), first identified as a TAP42 binding protein, acts as an inhibitor of the TOR signaling pathway by antagonizing TAP42 in yeast (Jacinto et al., 2001). Furthermore, yeast TIP41 can interact with the PP2A, PP4, and PP6 catalytic subunits (Gingras et al., 2005). TIPRL, the mammalian TIP41 ortholog, also demonstrates a similar ability to bind to α4 (the mammalian TAP42 ortholog) and the PP2A, PP4, and PP6 catalytic subunits (Nakashima and Tanimura-Ito, Oshiro, et al., 2013). The *A. thaliana* TIP41 protein showed a conserved interaction with the catalytic subunit of PP2A, but not with TAP46, in yeast two-hybrid assays (Punzo et al., 2018a). Interestingly, both TAP46 and TIP41 are involved in the ABA response in plants. TAP46 can interact with the ABA-regulated transcription factor ABA INSENSITIVE5 (ABI5), preventing PP2A protein phosphatases from dephosphorylating ABI5 and positively regulating the ABA response (Hu et al., 2014), while TIP41 directly interacts with PP2A and modulates the ABA response in *A. thaliana* (Punzo et al., 2018a). ABA signaling thus shows crosstalk with TOR signaling, and the components of TOR signaling may modulate the ABA response and drought tolerance.

In this study, we aimed to explore the functions of TaTIP41 and TaTAP46, two conserved components of the TOR signaling pathway, in drought tolerance regulation and the ABA response in wheat. We characterized *TaTIP41* homoeologs and demonstrated that the OE and RNA interference (RNAi)-mediated silencing of *TaTIP41* significantly altered drought tolerance and ABA-induced stomatal closure, indicating that TaTIP41 is a positive regulator of drought tolerance and the ABA response in wheat. Next, we confirmed that TaTIP41 physically interacts with TaTAP46 *in vivo*, and our transgenic assays indicated that TaTAP46 positively regulated drought tolerance and the ABA response in a manner similar to TaTIP41. Finally, we showed that both TaTIP41 and TaTAP46 interacted with the PP2A catalytic subunits to inhibit PP2A enzymatic activity and that silencing *TaPP2A-2* improved drought tolerance in wheat. Our findings provide new insights into the roles of TaTIP41 and TaTAP46 in drought tolerance and their potential application in the improvement of stress resistance in wheat.

RESULTS

Isolation and characterization of *TaTIP41* homoeologs in wheat

We isolated potential homoeologs of *TIP41*, a conserved component of TOR signaling, using a genome-wide bioinformatics analysis of *T. aestivum* cDNA sequences obtained from Ensembl plants (IWGSC, 2018). *TaTIP41* homoeologs located on chromosomes 5A, 5B, and 5D were identified as close homologs of the yeast and *A. thaliana TIP41* genes (Table S1). When we constructed a neighbor-joining phylogenetic tree by aligning the full-length TIP41 protein sequences from 21 plant species, *TIP41* genes were clustered into three subgroups: dicotyledons, monocotyledons, and green algae (Figure S1A). In particular, the conserved TIP41 domain shows high sequence and structural similarities among the eukaryotes, including mammals, plants, and yeast (Figure S1B, C), confirming that the TIP41 family is an evolutionarily conserved component of TOR signaling.

To characterize the *TaTIP41* homoeologs, we first investigated their subcellular localization patterns in wheat protoplasts or onion (*Allium cepa*) epidermal cells. The coding sequences (CDSs) of the *TaTIP41* homoeologs were fused in-frame with the gene encoding green fluorescent protein (GFP), and the resulting constructs were introduced into wheat protoplasts using the polyethylene glycol (PEG) method or into onion epidermal cells through particle bombardment (Li et al., 2016; Liu et al., 2020). The TaTIP41 homoeologs exhibited similar subcellular localization patterns; the GFP fluorescence of the TaTIP41-5A, -5B, and -5D fusion proteins was distributed throughout the cytoplasm and nucleus of the wheat protoplasts or onion epidermal cells (Figures 1A, S2).

Next, we examined the spatial and temporal expression patterns of the *TaTIP41* homoeologs using quantitative real-time PCR (qRT-PCR). The homoeologs exhibited similar expression patterns and were constitutively expressed in various wheat tissues at different developmental stages, but showed higher expression levels in young developing spikes (Figure 1B). To test whether *TaTIP41* expression is responsive to drought stress and ABA, we analyzed the expression of the *TaTIP41* homoeologs in seedling leaves over time in response to treatment with PEG and ABA. Compared with the control (0 h), both the PEG and ABA treatments induced higher expression of *TaTIP41* homoeologs (Figure 1C, D). After 48 h, the PEG treatment resulted in a two-fold increase in *TaTIP41-5A* expression (Figure 1C), while the ABA treatment induced its expression even more strongly (Figure 1D). By contrast, *TaTIP41-5D* exhibited slower and more durable responses to both treatments (Figure 1C, D). These PEG- and ABA-induced expression patterns suggested that TaTIP41 might participate in drought response and ABA signaling.

TaTIP41 acts as a positive regulator of wheat drought tolerance

To explore the biological functions of *TaTIP41* in wheat, we generated *TaTIP41-5D* OE and RNAi transgenic lines in the hexaploid wheat cultivar Fielder using *Agrobacterium tumefaciens*-mediated transformation (Wang et al., 2017).

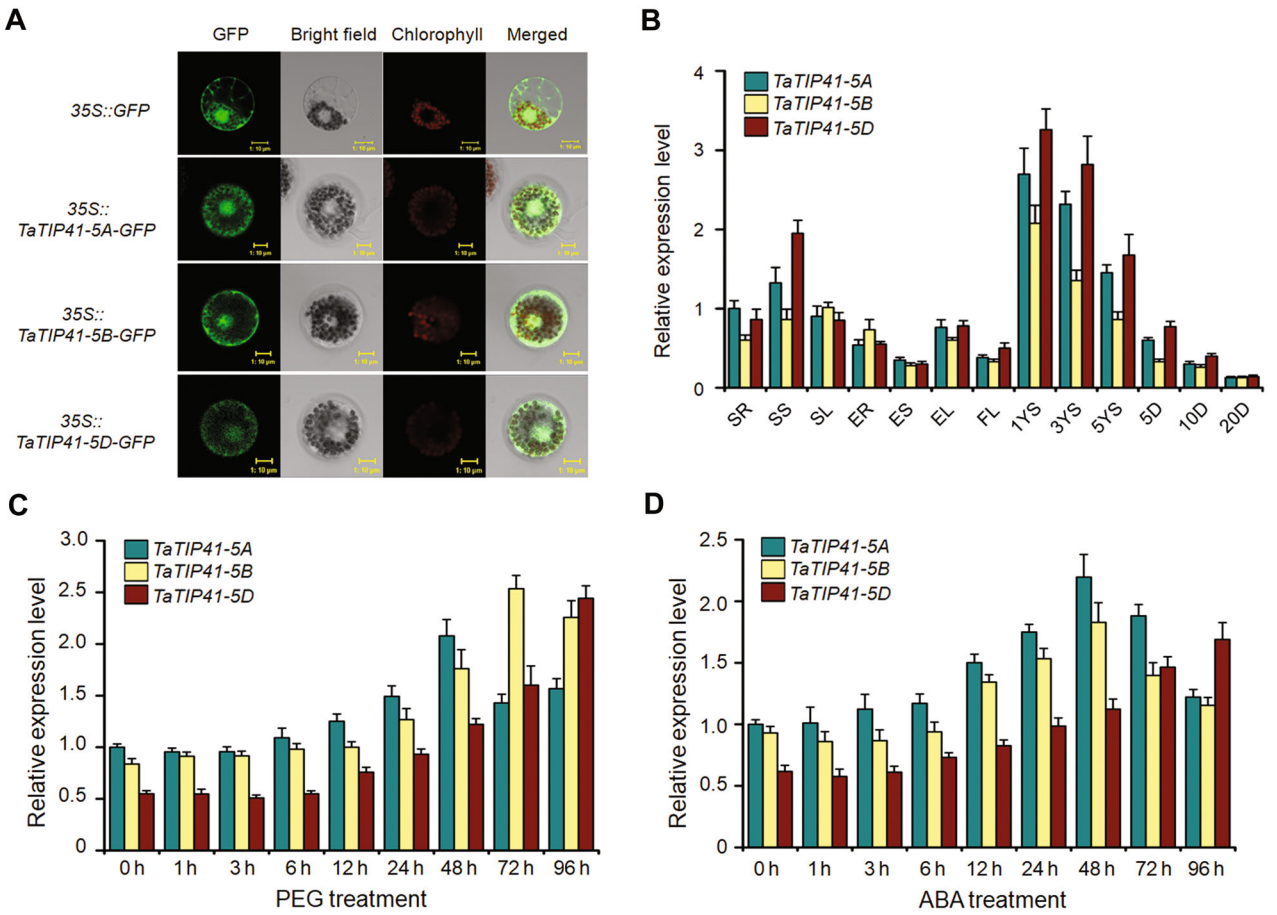

Figure 1. Characterization of *TaTIP41* homoeologs

(**A**) Subcellular localization of *TaTIP41* homoeologs in wheat protoplasts. Bars, 10 μm. (**B**) Spatial and temporal expression patterns of the *TaTIP41* homoeologs in wheat. SR, seedling roots; SS, seedling stems; SL, seedling leaves; ER, roots at elongation stage; ES, stems at elongation stage; EL, leaves at elongation stage; FL, flag leaves at heading stage; 1–5YS, young spikes of 1–5 cm in length; 5D–20D, grains at 5–20 d post anthesis. The values are presented as means ± *SD*. (**C, D**) The relative expression levels of *TaTIP41* homoeologs in wheat seedling leaves under PEG (**C**) and ABA (**D**) treatments. Wheat seedlings were treated with 15% PEG-6000 or 100 μM ABA for the indicated times. The values are presented as means ± *SD*.

Our analysis of the *TaTIP41* expression in the seedling leaves of the wild type (WT) control, OE, and RNAi transgenic lines using qRT-PCR demonstrated its upregulation in all three representative OE lines and downregulation in the three independent RNAi lines compared with the WT ($P < 0.01$ in both cases, Figure S3A, B).

Under normal growth conditions, we did not observe any obvious developmental differences among the WT, *TaTIP41* OE, and RNAi lines (data not shown); however, because *TaTIP41* expression is induced by PEG and ABA, it may be involved in regulating wheat drought tolerance. To test this possibility, we assayed WT and transgenic plants at the three-leaf stage for drought tolerance. Three representative *TaTIP41* OE lines, three representative RNAi lines, and WT plants were planted in one soil-containing pot to maintain the same drought stress conditions, and the soil relative water content (RWC) was measured at each point to evaluate drought conditions. All plants were grown to the three-leaf stage under well-watered conditions and then subjected to drought stress without watering. After 25 d of no watering (soil RWC = 43%), most leaves of the RNAi lines wilted, whereas only a few leaves of the OE lines and WT plants showed slight wilting (Figure 2A). After 35 d without watering (soil RWC = 36%), RNAi lines and WT plants showed severe dehydration, whereas only the OE lines showed a moderate dehydration phenotype (Figure 2A). After 5 d of rewatering (soil RWC = 85%), most OE plants resumed normal growth, and their survival rates were significantly higher than those of the WT plants; in contrast, the survival rates of the three RNAi lines were significantly lower than those of the WT plants (Figure 2B).

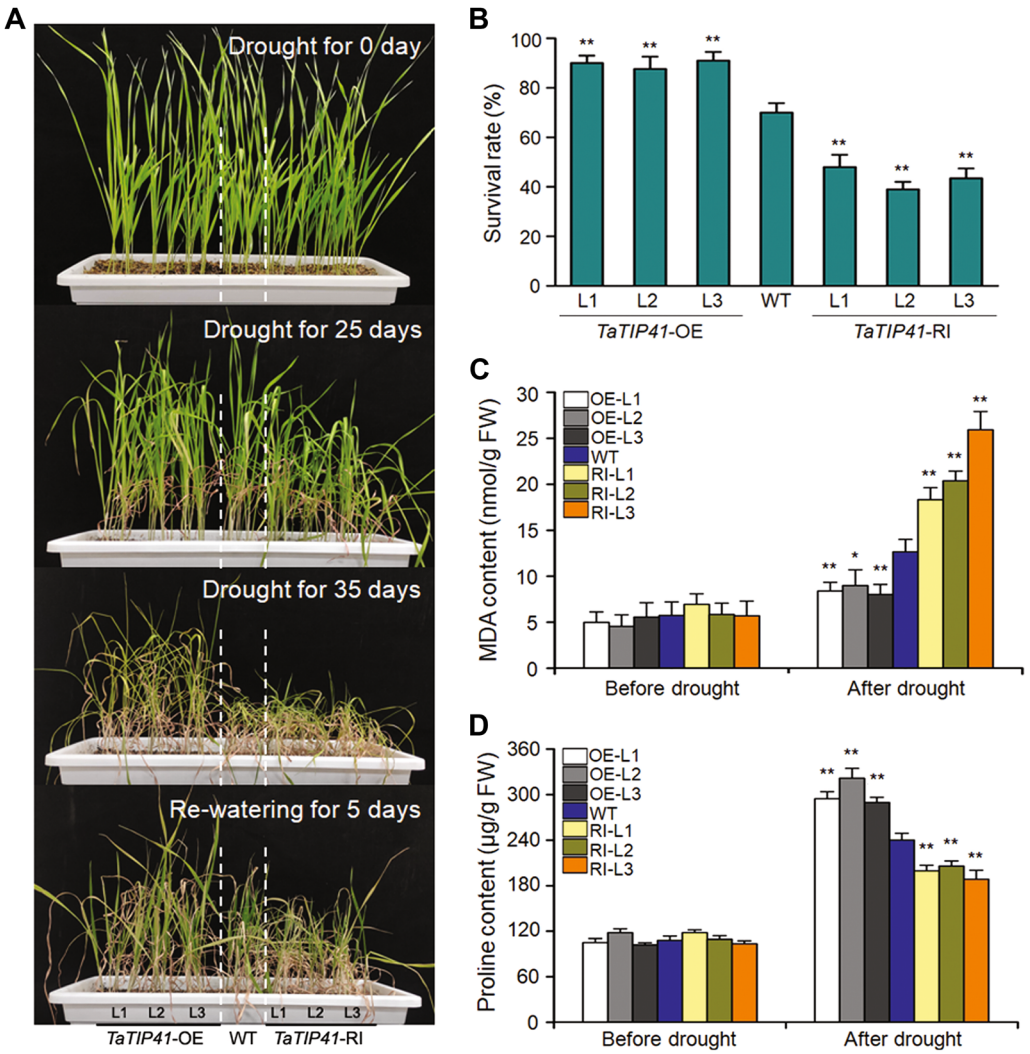

Figure 2. TaTIP41 is a positive regulator of drought tolerance in wheat

(**A**) Drought tolerance phenotypes of the wild type (WT), three *TaTIP41* overexpressing (OE-L1–L3) lines, and three *TaTIP41* RNAi (RI-L1–L3) lines. Wheat seedlings at the three-leaf stage were not watered for 0, 25, and 35 d, after which they were rewatered for 5 d. (**B**) Survival rates of the WT, *TaTIP41* OE-L1–L3, and RI-L1–L3 after drought stress. The values are presented as means ± SD. $^{**}P < 0.01$, indicating significant differences from the WT (analysis of variance [ANOVA]). (**C, D**) Malondialdehyde (MDA) content (**C**) and proline content (**D**) of WT, *TaTIP41* OE-L1–L3, and RI-L1–L3 after drought stress. FW, fresh weight. The values are presented as means ± *SD*. $^{*}P < 0.05$; $^{**}P < 0.01$, indicating significant differences from the WT (ANOVA).

In addition, the altered drought tolerance of the *TaTIP41* transgenic lines was correlated with changes in their malondialdehyde (MDA) and proline contents, two important parameters related to plant drought tolerance. Before drought stress, the MDA and proline contents showed no significant differences among the WT, OE, and RNAi lines (Figure 2C, D). After drought stress, the MDA content was higher in the RNAi lines but lower in the OE lines than in the WT ($P < 0.01$; Figure 2C). In contrast, the proline content was lower in the RNAi lines but significantly higher in the OE lines than in the WT under drought stress ($P < 0.01$; Figure 2D). Our results indicated that TaTIP41 positively regulates drought tolerance in wheat.

TaTIP41 positively regulates the ABA response to promote ABA-mediated stomatal closure

The rate of leaf water loss is a key factor determining plant drought tolerance. The water loss rate was measured using leaves from three representative *TaTIP41* OE lines, three representative RNAi lines, and WT plants. The OE lines lost water significantly more slowly than the WT leaves, while the RNAi lines showed faster water loss than the WT (Figure 3A). Due to the close relationship between ABA-mediated stomatal movement and the water loss rate under drought stress, we next observed stomatal movement in detached leaves of the RNAi line (RI-L1), OE line (OE-L1), and WT plants treated with different concentrations of ABA (0, 10, and 20 μM). There were no significant differences in stomatal apertures between the RI-L1, OE-L1, and WT plants under the 0 μM ABA treatment (Figure 3B, C), but with increasing ABA concentrations, the differences became evident. Under 20 μM ABA, the mean stomatal apertures of RI-L1 were approximately 1.5-fold and 3-fold higher than those of the WT and OE-L1, respectively (Figure 3B, C). These results indicated that TaTIP41 promoted ABA-mediated stomatal closure.

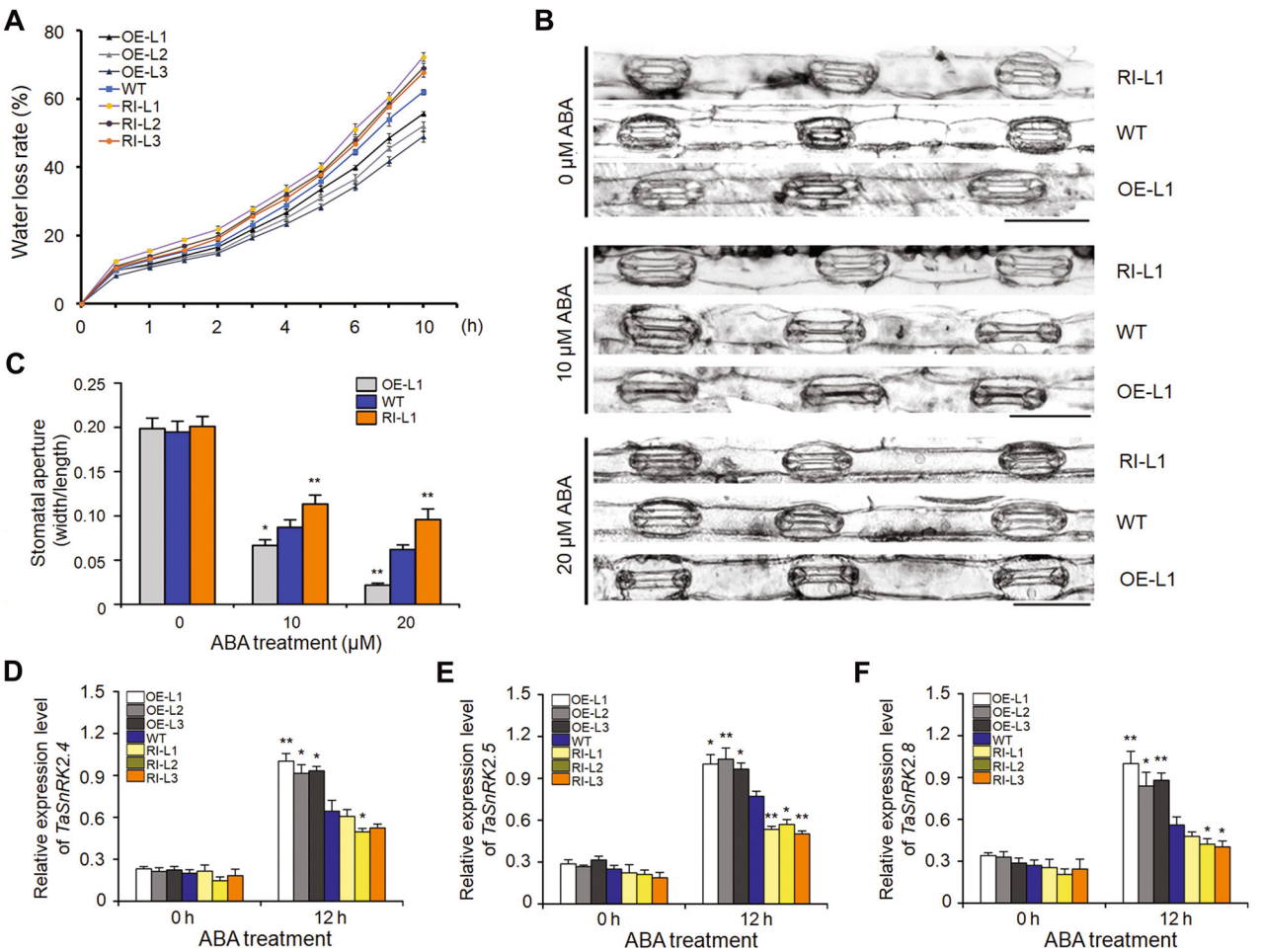

Figure 3. TaTIP41 positively regulates the ABA response in wheat

(**A**) Water loss rates of detached leaves from the wild type (WT), *TaTIP41* overexpressing (OE-L1–L3) lines, and *TaTIP41* RNAi lines (RI-L1–L3) at different time points. (**B**) ABA-induced stomatal closure in WT, OE-L1, and RI-L1. Stomata were observed in leaf epidermis treated with 0, 10, or 20 μM ABA. Bars, 50 μm. (**C**) Stomatal aperture (width/length) of WT, OE-L1, and RI-L1 treated with 0, 10, or 20 μM ABA. The values are presented as means ± *SD*. $^*P < 0.05$; $^{**}P < 0.01$, indicating significant differences from the WT (analysis of variance [ANOVA]). (**D**–**F**) Comparison of ABA-responsive gene expression levels among WT, *TaTIP41* OE-L1–L3, and RI-L1–L3 in response to treatment with 100 μM ABA. The values are presented as means ± *SD*. $^*P < 0.05$; $^{**}P < 0.01$, indicating significant differences from the WT (ANOVA).

We further examined the expression levels of some ABA-responsive genes, including *TaSnRK2.4*, *TaSnRK2.5*, and *TaSnRK2.8* (Ma et al., 2022), in the seedling leaves of three *TaTIP41* OE lines, three RNAi lines, and WT plants. Before an ABA (100 μM) treatment (0 h), none of the three genes was differentially expressed among the different genotypes; however, after 12 h of ABA treatment, all three showed significantly higher expression levels in the OE lines and lower expression levels in the RNAi lines than in the WT plants (Figure 3D–F). These results indicate that TaTIP41 positively regulates the ABA response, possibly by enhancing the expression of ABA-responsive genes.

TaTIP41 interacts with TaTAP46 in plant cells

In yeast, TIP41 participates in TOR signaling by interacting with the PP2A regulatory subunit TAP42 (Jacinto et al., 2001). As the plant TIP41/TAP46 and yeast TIP41/TAP42 proteins are conserved, we speculated that TIP41 could also interact with TAP46 in plants. To confirm the interaction between TaTIP41 (TraesCS5D02G407600) and TaTAP46 (TraesCS5D02G142100), we performed a firefly luciferase complementation imaging (LCI) assay and bimolecular fluorescence complementation (BiFC) assay in tobacco (*Nicotiana benthamiana*) leaves. The LCI assay revealed luciferase luminescence following the co-infiltration of the leaves with TaTIP41-nLUC and cLUC-TaTAP46 (Figure 4A), indicating a strong interaction between TaTIP41 and TaTAP46 in

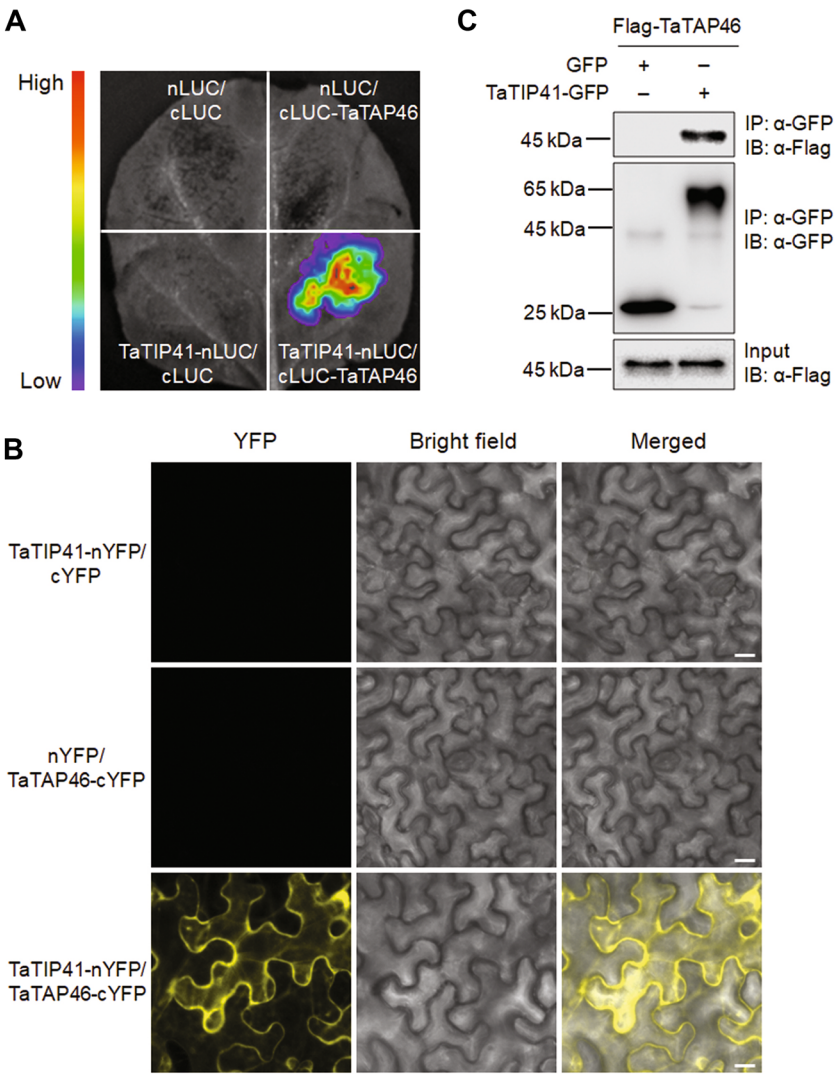

Figure 4. TaTIP41 physically interacts with TaTAP46

(**A**) Luciferase complementation imaging (LCI) assay showing physical interaction of TaTIP41 with TaTAP46 in *Nicotiana benthamiana* leaves. nLUC, N-terminal of LUC; cLUC, C-terminal of LUC. (**B**) Bimolecular fluorescence complementation (BiFC) assay showing the interaction between TaTIP41 and TaTAP46 in *N. benthamiana* leaf epidermal cells. nYFP, N-terminal portion of YFP; cYFP, C-terminal portion of YFP. Bars, 20 μm. (**C**) Co-immunoprecipitation (Co-IP) assay in *N. benthamiana* leaves showing the *in vivo* interaction between TaTIP41 and TaTAP46. TaTIP41-GFP and Flag-TaTAP46 were immunoprecipitated with agarose-conjugated anti-GFP monoclonal antibodies, and the immunoblots were detected with anti-GFP or anti-Flag antibodies. The GFP empty vector was used as a negative control.

plant cells. Similar results were obtained using the BiFC assay: A strong YFP signal was detected in the cytoplasm and cell membrane of tobacco leaf cells co-infiltrated with TaTIP41-nYFP and TaTAP46-cYFP (Figure 4B), whereas the YFP signal was negligible in the negative controls. In addition, a co-immunoprecipitation (Co-IP) assay showed that the Flag-TaTAP46 protein could be co-precipitated with TaTIP41-GFP protein, but not the GFP control (Figure 4C), further confirming the interaction between TaTIP41 and TaTAP46 *in vivo*. These results suggest that TaTIP41 physically interacts with TaTAP46 in plant cells.

TaTAP46 positively regulates wheat drought tolerance

As a TaTIP41-interacting partner, TaTAP46 might also be involved in the regulation of wheat drought tolerance. To test this hypothesis, we first determined whether *TaTAP46* expression is responsive to drought stress and ABA. As expected, both PEG and ABA induced the expression of *TaTAP46* (Figure S4A, B). Next, we generated *TaTAP46-5D* OE and RNAi lines in the hexaploid wheat cultivar Fielder using a similar method as for *TaTIP41* and verified *TaTAP46* expression levels in three independent *TaTAP46* OE and RNAi lines (Figure S5A, B). To evaluate drought tolerance, we subjected WT and transgenic plants at the three-leaf stage to a water deficit treatment, as described earlier. After 22 d without watering (soil RWC = 45%), the RNAi lines showed obvious water stress, with most leaves rolled, whereas WT and OE plants remained green with limited rolling and wilting (Figure 5A). After 30 d without watering (soil RWC = 37%), the RNAi lines showed more severe dehydration, while the OE lines showed less dehydration compared with the WT (Figure 5A). After 5 d of rewatering (soil RWC = 79%), most RNAi plants failed to recover, resulting in an approximate 29%–41% survival rate, which was significantly lower than that of the WT (77% survival rate); by contrast, more than 90% of the OE plants survived and recovered normal growth (Figure 5B). In addition, the MDA and proline contents were consistent with the phenotype and survival rates. After drought stress,

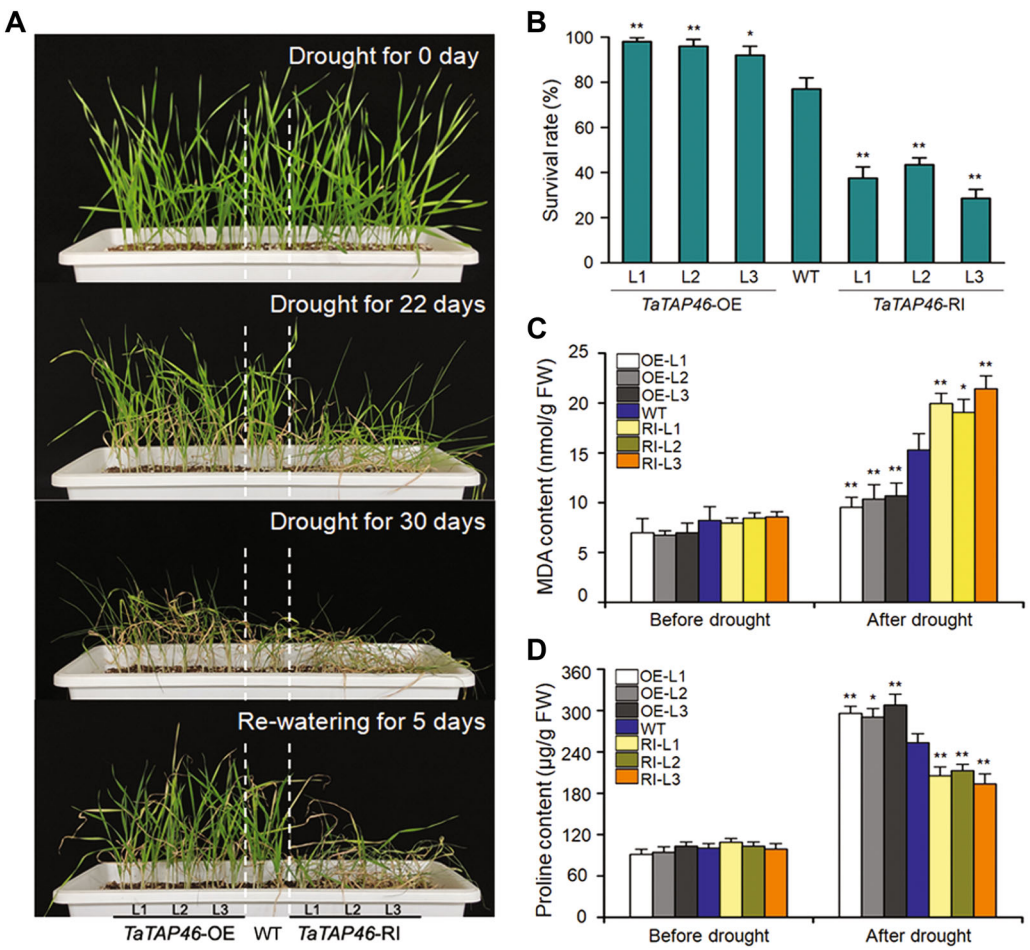

Figure 5. TaTAP46 is a positive regulator of drought tolerance in wheat

(**A**) Drought tolerance phenotypes of the wild type (WT), three *TaTAP46* overexpressing lines (OE-L1–L3), and three *TaTAP46* RNAi (RI-L1–L3) lines. Wheat seedlings at the three-leaf stage were not watered for 0, 22, and 30 d, and then rewatered for 5 d. (**B**) Survival rates of the WT, *TaTAP46* OE-L1–L3, and RI-L1–L3 after drought stress. The values are presented as means ± *SD*. $*P < 0.05$; $**P < 0.01$, indicating significant differences from the WT (analysis of variance [ANOVA]). (**C, D**) Malondialdehyde (MDA) content (**C**) and proline content (**D**) of the WT, *TaTAP46* OE-L1–L3, and RI-L1–L3 after drought stress. The values are presented as means ± *SD*. $*P < 0.05$; $**P < 0.01$, indicating significant differences from the WT (ANOVA).

the RNAi lines had significantly higher MDA and lower proline contents, whereas the OE lines had significantly lower MDA and higher proline contents than the WT plants (Figure 5C, D). These results suggest that TaTAP46 is a positive regulator of wheat drought tolerance, similar to TaTIP41.

TaTAP46 positively regulates the ABA response like TaTIP41

To test whether TaTAP46 is involved in the ABA response like TaTIP41, we compared the stomatal movement of detached leaves from the *TaTAP46* RNAi line (RI-L1), OE line (OE-L1), and WT plants treated with different concentrations of ABA (0, 10, and 20 μM). Under the 10 and 20 μM ABA treatments, the RI-L1 plants exhibited larger stomatal apertures than the WT, while the OE-L1 plants had narrower stomatal apertures (Figure 6A, B). We also investigated the expression levels of the ABA-responsive genes *TaSnRK2.4*, *TaSnRK2.5*, and *TaSnRK2.8* in the seedling leaves of the various genotypes under an ABA (100 μM) treatment. After 12 h of ABA treatment, all three genes showed significantly higher expression levels in the OE lines and lower expression levels in the RNAi lines than in the WT (Figure 6D–F). These results indicate that TaTAP46 positively regulates the ABA response, like TaTIP41, by promoting ABA-mediated stomatal closure and enhancing the expression of ABA-responsive genes.

Both TaTIP41 and TaTAP46 inhibit PP2A activity via their interaction with PP2A catalytic subunits

Previous studies have indicated that TAP46 and TIP41 are PP2A-associated proteins in plants (Ahn et al., 2011; Punzo et al., 2018a). To validate the interaction between PP2As and TaTIP41 or TaTAP46, we cloned three representative PP2A catalytic subunits, TaPP2A-1 (TraesCS7D02G358600), TaPP2A-2 (TraesCS5D02G465400), and TaPP2A-3 (TraesCS 6D02G171400), and used them in a protein–protein interaction assay. The LCI assays showed that all three TaPP2As could

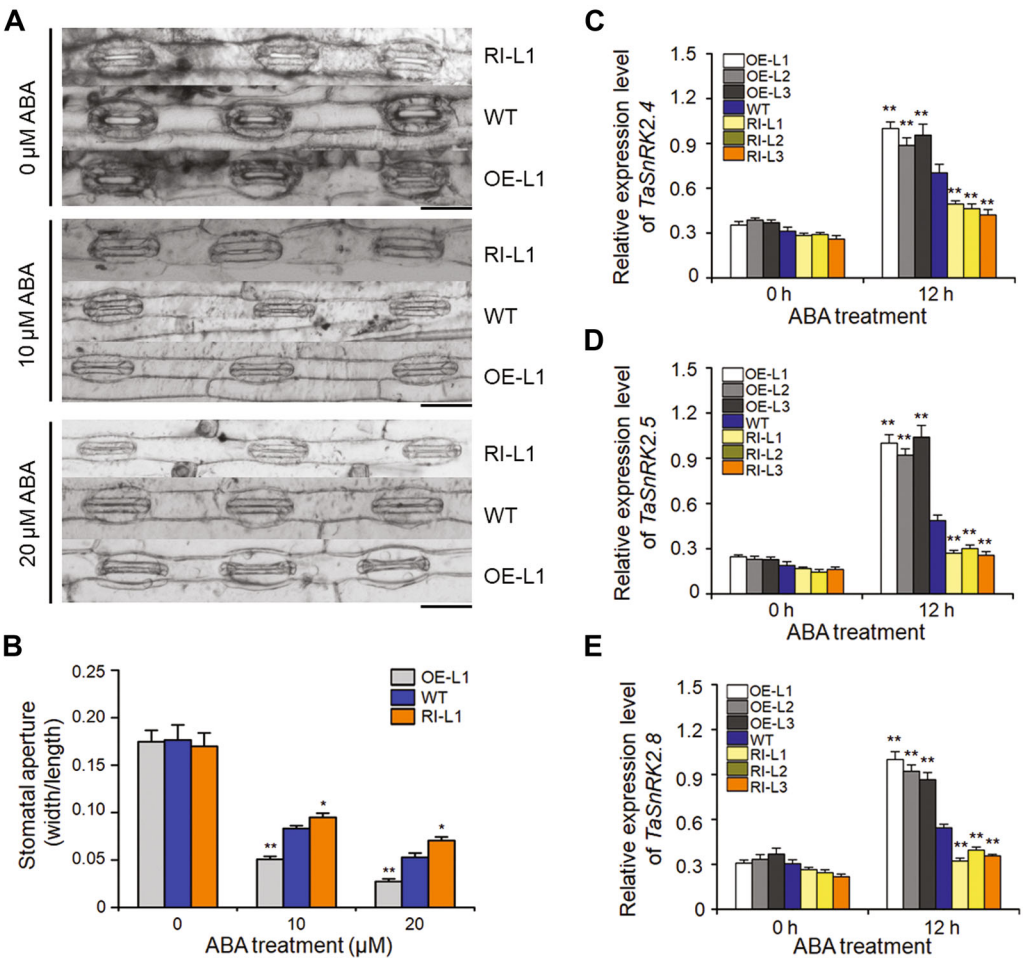

Figure 6. TaTAP46 positively regulates the ABA response in wheat

(**A**) ABA-induced stomatal closure in the wild type (WT), *TaTAP46* overexpressing (OE-L1) line, and *Ta-TAP46* RNAi (RI-L1) line. Stomata were observed in the leaf epidermis treated with 0, 10, or 20 μM ABA. Bars, 50 μm. (**B**) Stomatal aperture (width/length) of the WT, OE-L1, and RI-L1 treated with 0, 10, or 20 μM ABA. The values are presented as means ± *SD*. $^{*}P < 0.05$; $^{**}P < 0.01$, indicating significant differences from the WT (analysis of variance [ANOVA]). (**C**–**E**) Comparison of the expression levels of the ABA-responsive genes (*TaSNRK2.4*, *TaSNRK2.5*, and *TaSNRK2.8*, respectively) among the WT, *TaTAP46* OE-L1–L3, and RI-L1–L3 lines in response to treatment with 100 μM ABA. The values are presented as means ± *SD*. $^{**}P < 0.01$, indicating significant differences from the WT (ANOVA).

interact with TaTIP41 and TaTAP46 (Figures 7A, B, S6A–D). Co-infiltration of TaTIP41-nLUC and cLUC-TaPP2A-2 or TaPP2A-2-nLUC and cLUC-TaTIP41 resulted in effective luminescence generated by the complemented luciferase (Figure 7A, B). Further evidence was obtained through BiFC assays, which revealed YFP signals in the tobacco leaf cells co-infiltrated with TaPP2As-nYFP and TaTIP41-cYFP or TaTAP46-cYFP (Figures 7C, S6E), indicating that both TaTIP41 and TaTAP46 interacted with the TaPP2As in plant cells. To further map the interaction regions of TaPP2As with TaTIP41 and TaTAP46, we divided the full-length TaPP2A-2 protein into two parts: the N-terminal region (residues 1–192) and the C-terminal region (residues 170–307) (Figure 7D). LCI assays using these two truncated TaPP2A-2 constructs revealed that the N-terminal and C-terminal regions mediated the interaction with TaTAP46 and TaTIP41, respectively (Figure 7E, F). Thus, TaPP2As might interact with TaTIP41 and TaTAP46 simultaneously due to their different interactive regions.

As PP2A interaction partners, TIP41 and TAP46 modulate PP2A activity in plants (Ahn et al., 2011; Hu et al., 2014; Punzo et al., 2018a); therefore, we examined the total PP2A activity in the WT and the *TaTIP41* and *TaTAP46* transgenic lines. Under normal conditions, the total PP2A activity was slightly reduced in the *TaTIP41* and *TaTAP46* OE lines, but significantly increased in the *TaTIP41* and *TaTAP46* RNAi lines compared with the WT control (Figure 8A). After the drought treatment, the total PP2A activity was reduced in all WT, *TaTIP41*, and *TaTAP46* transgenic lines; however, the *TaTIP41* and *TaTAP46* OE lines had significantly lower PP2A activity, while the RNAi lines had significantly higher PP2A activity compared with the WT control (Figure 8A). The negative correlation between PP2A activity and *TaTIP41* or

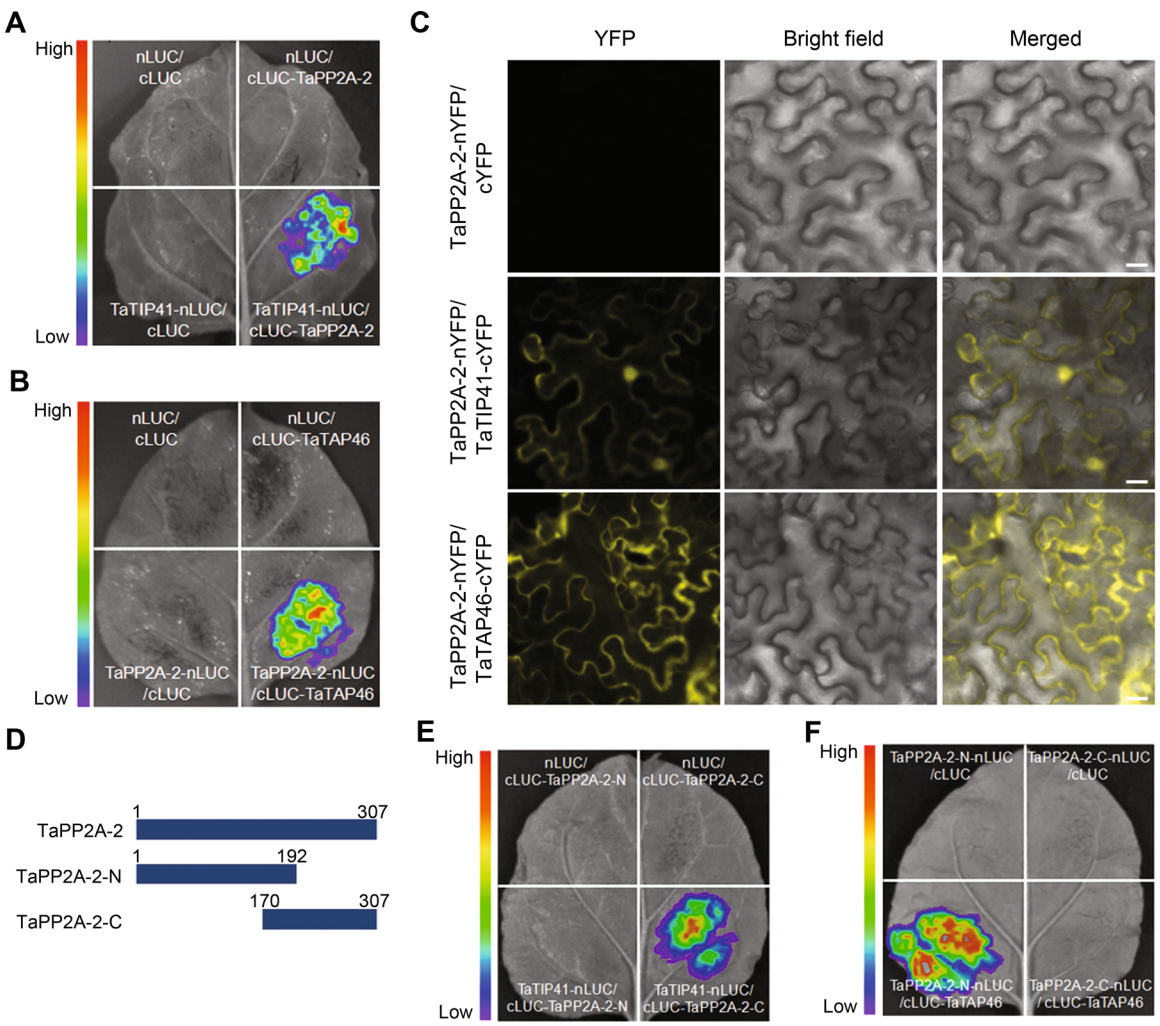

Figure 7. Both TaTIP41 and TaTAP46 physically interact with TaPP2A-2

(**A, B**) Luciferase complementation imaging (LCI) assays showing that TaPP2A-2 interacts with both TaTIP41 (**A**) and TaTAP46 (**B**) in *Nicotiana benthamiana* leaves. (**C**) Bimolecular fluorescence complementation (BiFC) assay showing the interaction between TaPP2A-2 and TaTIP41 or TaTAP46 in *N. benthamiana* leaf epidermal cells. Bars, 20 μm. (**D**) Schematic diagrams representing the full-length and truncated TaPP2A-2 proteins. (**E, F**) LCI assays showing that the C-terminal region of TaPP2A-2 interacts with TaTIP41 (**E**) and the N-terminal region of TaPP2A-2 interacts with TaTAP46 (**F**) in *N. benthamiana* leaves.

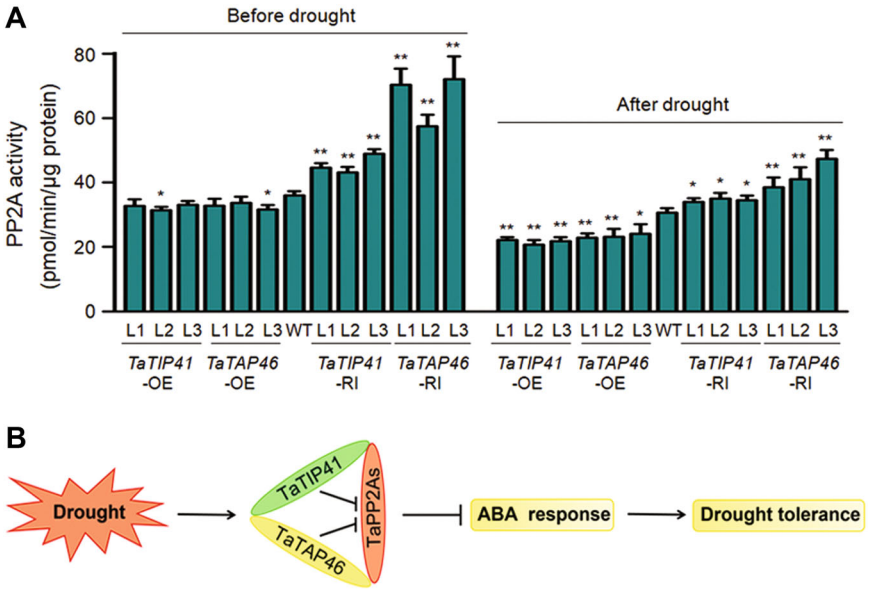

Figure 8. Both TaTIP41 and TaTAP46 inhibit PP2A activity in wheat

(**A**) Measurement of the total PP2A activity in seedlings of the wild type (WT), *TaTIP41* overexpressing (OE), *TaTIP41* RNAi (RI), *TaTAP46* OE, and *TaTAP46* RI lines before and after drought stress. The values are presented as means ± *SD*. $^{*}P < 0.05$; $^{**}P < 0.01$, indicating significant differences from the WT (analysis of variance). (**B**) A proposed working model for the functions of TaTIP41 and TaTAP46 in drought tolerance. The line with a bar indicates negative regulation, and arrows indicate positive regulation. Drought can induce the expression of *TaTIP41* and *TaTAP46*; *TaTIP41*, TaTAP46, and TaPP2A may form a heterotrimer due to their mutual interactions with each other. Both TaTIP41 and TaTAP46 inhibit PP2A activity, and their inhibitory effects on PP2A activity may enhance the ABA response and drought tolerance in wheat.

TaTAP46 expression levels suggested that both TaTIP41 and TaTAP46 act as repressors of PP2A activity via interactions with the PP2A catalytic subunits.

Silencing *TaPP2A-2* in wheat increases drought tolerance

To further explore the function of the PP2A catalytic subunits in drought tolerance, we used a virus-induced gene silencing system based on the barley stripe mosaic virus (BSMV-VIGS) to silence *TaPP2A-2* in wheat seedlings. To control the drought conditions, control (1× FES buffer), negative control (BSMV::γ_0), and *TaPP2A-2*-silenced (BSMV::*TaPP2A-2*) plants were planted in one pot. After the positive control plants (BSMV::*TaPDS*) showed severe photobleaching, all the plants were subjected to drought stress by discontinuing watering for 15 d and then rewatered for 5 d (Figure S7A, B). The phenotypic comparisons and survival rates demonstrated that silencing *TaPP2A-2* improved drought tolerance in wheat (Figure S7B, C). Consistent with these results, the *TaPP2A-2* expression level and the total PP2A enzymatic activity were significantly reduced in the BSMV::*TaPP2A-2* plants compared with the other controls before and after drought stress (Figure S7D, E). *TaPP2A-2* expression and the total PP2A enzymatic activity were downregulated by drought stress (Figure S7D, E). In addition, we examined the expression of the ABA-responsive genes *TaSnRK2.4*, *TaSnRK2.5*, and *TaSnRK2.8* and found that their relative expression levels were all significantly higher in the BSMV::*TaPP2A-2* plants than in the control plants after drought stress (Figure S7F). These data indicate that TaPP2A-2 negatively regulates wheat drought tolerance.

DISCUSSION

TaTIP41 and TaTAP46 are two novel positive regulators of drought tolerance in wheat

In yeast, TIP41 was identified as a TAP42 binding protein that antagonizes TAP42 in TOR signaling (Jacinto et al., 2001). Although TIP41 is highly conserved among eukaryotes, including mammals, plants, and yeast (Figure S1), plant TIP41 was originally used as a reference gene in expression assays because of its ubiquitous expression (Czechowski et al., 2005). Recent studies in *A. thaliana* have indicated that *TIP41* is involved in the ABA response (Punzo et al., 2018a, b); however, information on *TIP41* functions under environmental stresses, such as drought, is limited. In this study, we first characterized *TaTIP41* homoeologs in wheat and demonstrated that their expression was induced by PEG and ABA treatments (Figure 1A–D), implying that *TaTIP41* might have a role in wheat drought tolerance. We therefore generated *TaTIP41* OE and RNAi transgenic lines, which were more and less drought tolerant than the WT, respectively (Figure 2A–D). We inferred that TaTIP41 is a novel positive regulator of drought tolerance in wheat. ABA-mediated stomatal closure is central to water loss rate and drought tolerance in plants (Mao et al., 2022b). In our study, *TaTIP41* OE promoted ABA-mediated stomatal closure, whereas *TaTIP41* RNAi had the

opposite effect (Figure 3B, C). Moreover, some ABA-responsive genes had higher expression levels in the *TaTIP41* OE lines than in the WT and RNAi lines following an ABA treatment (Figure 3D–F). Taken together, these results indicate that TaTIP41 positively regulates drought tolerance in wheat, mainly by promoting the ABA response.

A previous study failed to confirm an interaction between TIP41 and TAP46 in *A. thaliana* using yeast two-hybrid assays (Punzo et al., 2018a). To rule out possible false-negative results in this yeast system, we performed LCI, BiFC, and Co-IP assays in tobacco leaves to determine whether TaTIP41 associates with TaTAP46 *in vivo*. Indeed, all three assays pointed to a strong interaction between TaTIP41 and TaTAP46 in plant cells (Figure 4A–C), providing the first evidence of such an interaction in plants. We also generated *TaTAP46* OE and RNAi transgenic lines and investigated their drought tolerance phenotypes, revealing stronger and weaker drought tolerances than the WT to drought stress, respectively (Figure 5A–D). Consistent with this, *TaTAP46* OE showed a stronger ABA response than the WT and RNAi lines (Figure 6A–E). These results demonstrated that *TaTAP46* also acts as a positive regulator of drought tolerance and the ABA response in wheat. Interestingly, TaTIP41 and TaTAP46 have similar functions in drought tolerance, notwithstanding their antagonistic roles in TOR signaling (Jacinto et al., 2001). Collectively, these results led us to infer that the relationship between TaTIP41 and TaTAP46 is likely to vary between environmental conditions and signaling pathways; however, further studies are required to elucidate the mechanisms underlying the complex relationship between TaTIP41 and TaTAP46.

TaTIP41 and TaTAP46 are both conserved PP2A interaction partners and modulate PP2A activity in wheat

PP2A, a major member of the Ser/Thr phosphatase family, plays a crucial role in plant development and stress responses (Janssens and Goris, 2001; Li et al., 2019). PP2As are heterotrimeric holoenzyme complexes comprising scaffolding, regulatory, and catalytic subunits. Accumulating evidence has revealed complicated roles for these proteins in ABA signaling. In *A. thaliana*, the PP2A catalytic subunit PP2Ac-2 is a negative regulator of ABA signaling, as the *pp2ac-2* mutant loses water more slowly than the WT due to its increased ABA sensitivity (Pernas et al., 2007). In contrast, several PP2A-type regulatory subunits interact with SnRK2-type protein kinases, positively regulating ABA signaling in seed germination and stomatal closure and negatively regulating ABA signaling in root growth (Waadt et al., 2015). Thus, the exact regulatory mechanisms of the PP2As in ABA signaling have yet to be fully elucidated (Yang et al., 2017).

As a conserved PP2A interaction partner, TIP41 interacts with PP2A catalytic subunits in yeast, mammals, and plants (Gingras et al., 2005; Nakashima and Tanimura-Ito, Oshiro, et al., 2013; Punzo et al., 2018a). TAP46 is a regulatory subunit of PP2A and interacts with multiple PP2A catalytic subunits in plants (Ahn et al., 2011). In this study, we confirmed that both TaTIP41 and TaTAP46 physically interact with PP2A catalytic subunits in wheat, including TaPP2A-1, TaPP2A-2, and TaPP2A-3 (Figures 7A–C, S6A–D), indicating a conserved mutual interaction between the TaTIP41, TaTAP46, and PP2A catalytic subunits. In addition, the total PP2A activity was significantly increased in the *TaTIP41* and *TaTAP46* RNAi lines, and decreased in *TaTIP41* and *TaTAP46* OE lines, especially after drought stress (Figure 8A). Consequently, both TaTIP41 and TaTAP46 might inhibit PP2A activity via interaction with PP2A catalytic subunits. Interestingly, the N-terminal and C-terminal regions of TaPP2A-2 interacted with TaTAP46 and TaTIP41, respectively (Figure 7E, F), suggesting that TaTIP41, TaTAP46, and TaPP2A-2 might form a complex. In mammals, the PP2A catalytic subunit forms a heterotrimer with TIPRL (ortholog of yeast TIP41) and α4 (ortholog of yeast TAP42), and TIPRL directly inhibits PP2Ac activity *in vitro* (Smetana and Zanchin, 2007). In *A. thaliana*, TAP46 represses PP2A activity and positively regulates ABA signaling by preventing PP2A-mediated dephosphorylation of ABI5 (Hu et al., 2014). Consistent with its negative effect on ABA signaling, silencing *TaPP2A-2* improved the drought tolerance and ABA response of wheat seedlings (Figure S4); we therefore inferred that TaTIP41 and TaTAP46 might interact with the PP2A catalytic subunits and inhibit PP2A activity to positively affect ABA signaling and drought tolerance in wheat.

Based on our findings, we propose a working model for the roles of TaTIP41 and TaTAP46 in the regulation of wheat drought tolerance (Figure 8B). Mutual interactions exist among TaTIP41, TaTAP46, and the TaPP2As, possibly forming a heterotrimer complex to fine-tune TaPP2A activity. ABA signaling or drought stress induces both *TaTIP41* and *TaTAP46*, which repress the activity of TaPP2As to promote the ABA response and increase drought tolerance in wheat. This model provides insights into a novel regulatory module for drought tolerance; however, further genetic evidence is needed.

TOR signaling is an important pathway in environmental adaptation but is not fully exploited in crops

TOR signaling plays a pivotal role in sensing and responding to nutrient availability, cellular energy status, and stress and growth stimuli in all eukaryotes (Wullschleger et al., 2006; Liu and Xiong, 2022). Despite the high conservation of the core components of TOR signaling, the plant TOR signaling network evolves specific functions on sensing light, phytohormones, and inorganic nutrients for adaptation to plant-specific biological processes (Liu and Xiong, 2022). Recently, previously unknown plant TOR targets have been identified, such as the BZR1 and EIN2 transcription factors, which are involved in the regulation of plant growth and stress responses (Zhang et al., 2016; Fu et al., 2021). Furthermore, plant TOR signals can be activated or inhibited by many abiotic and biotic stresses, and TOR signaling shows a wide

interaction with stress-related phytohormones, including ABA, salicylic acid, jasmonic acid, and ethylene, indicative of its key role in environmental adaptation (Liu and Xiong, 2022). Expanding the TOR signaling network in the plant responses to stress may uncover novel regulatory mechanisms for plant sensing and stress tolerance to modulate their growth and development. Unfortunately, TOR signaling has not been well exploited in crops, and little information is available on its involvement in the resistance to various environmental stresses, such as drought, salinity, and heat.

Due to the lack of molecular and biochemical assays for TOR signaling in crops, previous studies mainly focused on the TOR kinase rather than other components of the process. TaTIP41 and TaTAP46 were regarded as two putative evolutionarily conserved components of TOR signaling based on their high sequence and structure similarities among eukaryotes (Figure S1). Here, we showed that TaTIP41 and TaTAP46 are positive regulators of wheat drought tolerance and the ABA response (Figures 2, 5), indicating a role for TOR signaling in drought tolerance. Further studies will be needed to reveal the relationship between other components of TOR signaling and drought tolerance in wheat. In addition, a previous study has shown that TaTAP46 is a positive regulator of grain weight in wheat and that the favorable *TaTAP46-5A* haplotype is associated with higher grain weights (Zhang et al., 2021); thus, TOR signaling also contributes to grain development and yield traits. Taking into consideration its fundamental role in plant growth, development, and the response to environmental stresses, the study of TOR signaling in crops may facilitate its potential application in crop improvement for yield enhancement and environmental adaptability.

MATERIALS AND METHODS

Plant materials and treatments

Two common wheat (*Triticum aestivum* L.) accessions, cv. Chinese Spring (CS) and cv. Fielder, were used in this study. CS was used for the gene isolation and expression analysis, while Fielder was used for the genetic transformation experiments. For the PEG and ABA treatments, the germinated CS seeds were cultivated in Hoagland solution in a growth chamber at 20°C (day) and 15°C (night) in a 16-h light/8-h dark photoperiod. At the two-leaf stage, the seedlings were transferred into Hoagland solution containing 15% PEG-6000 or 100 μM ABA. The leaf tissues of treated plants were collected at the indicated time points, immediately frozen in liquid nitrogen, and stored at –80°C until further use.

RNA extraction and qRT-PCR

Total RNA was extracted from various wheat tissues using the RNAprep Pure Plant Kit (Tiangen Biotech, Beijing, China), and cDNA was synthesized using a FastQuant RT Kit (Tiangen Biotech). The qRT-PCR was carried out on an Applied Biosystems 7500 Real-time PCR system (Thermo Fisher Scientific, USA) using SYBR Premix Ex Taq (Takara Bio, Japan), as described by Liu et al. (2020). The wheat *Tubulin* gene was used as the internal reference (Ma et al., 2022). The relative expression level of each gene was calculated as a fold-change value using the comparative CT method (Livak and Schmittgen, 2001). All assays were performed in triplicate in independent experiments. The primers used in this study are listed in Table S1.

Subcellular localization

The full-length CDSs of the *TaTIP41* homoeologs were amplified from CS cDNA samples and cloned into the pJIT163-GFP vector, as previously described (Liu et al., 2020). The resulting constructs and the control vector were introduced into wheat mesophyll protoplasts via a PEG-mediated method (Liu et al., 2020) or into onion epidermal cells by particle bombardment (Li et al., 2016). After a 16-h incubation, the GFP fluorescence was observed using an LSM880 confocal laser-scanning microscope (Carl Zeiss, Germany).

Vector construction and plant transformation

To construct the *TaTIP41* OE vector, the full-length CDS of *TaTIP41-5D* (*TraesCS5D02G407600*) was amplified from a CS seedling cDNA sample and cloned into a modified pCAMBIA3301 vector under the control of the maize *Ubi* promoter (Liu et al., 2020). For the *TaTIP41* RNAi construct, a 379-bp sequence derived from the *TaTIP41-5D* CDS (nucleotides 122–500) was amplified and sequentially cloned into the *Bam*HI/*Kpn*I and *Sac*I/*Spe*I sites of the pWMB006 vector. The resulting construct was double-digested using *Hind*III and *Eco*RI and then cloned into the corresponding sites of the pCAMBIA3301 vector to generate the *TaTIP41* RNAi construct. Similarly, the full-length CDS of *TaTAP46-5D* (*TraesCS5D02G142100*) and a 405-bp sequence from the *TaTAP46-5D* CDS (nucleotides 612–1,016) were used to generate the *TaTAP46* OE and RNAi constructs, respectively. All constructs were introduced into the *Agrobacterium tumefaciens* strain EHA105 and transformed into cv. Fielder, following a modified *A. tumefaciens*-mediated transformation method (Wang et al., 2017). The T_3 generations of the transgenic lines were used for the phenotypic assessment.

Assays of drought tolerance and water loss rate

The transgenic lines and the WT control were planted in a single plastic box (43.0 cm × 19.0 cm × 14.0 cm) filled with soil in a growth chamber at 20°C (day) and 15°C (night) in a 16-h light/8-h dark photoperiod. For the drought tolerance assay, seedlings at the three-leaf stage were not watered for approximately 30 d and then rewatered for 5 d. The soil RWC was measured to evaluate drought conditions following a previously described method (Ma et al., 2022). Phenotypes before and after the drought treatment were surveyed and photographed. The surviving plants of each line were counted, and the survival rate was determined. For the leaf water loss assay, detached leaves from 30-d-old wheat

plants were exposed to air, dehydrated at room temperature, and weighed at the indicated times to calculate the rate of water loss (Mao et al., 2022b). All experiments were repeated three times, and representative results are shown.

Measurements of the proline and MDA contents

To measure the proline content, approximately 0.3 g wheat leaf was homogenized using 3% (w/v) sulfosalicylic acid, and the homogenate was centrifuged at 10,000 *g* for 5 min. The supernatant (2 mL) was mixed with 2 mL glacial acetic acid and 2 mL acid ninhydrin, and the mixture was incubated in boiling water for 1 h. Then, 4 mL toluene was added to the mixture, and its absorbance at 520 nm was measured using a UV spectrometer (UV-2600; Shimadzu, Japan). A calibration curve was used to determine the proline content (Bates et al., 1973). For measurements of the MDA content, approximately 0.3 g wheat leaf was homogenized using 5 mL phosphate buffer (pH 7.8) and then centrifuged at 10,000 *g* for 20 min at 4°C to obtain the supernatant. A mixture of 2 mL supernatant and 5 mL 0.5% thiobarbituric acid was incubated in boiling water for 15 h and then centrifuged at 4,000 *g*. The MDA content was calculated using the absorption values at 600, 532, and 450 nm, as described previously (Zheng et al., 2008).

Stomatal aperture analysis

The stomatal apertures were measured as previously described (Ma et al., 2022). In brief, wheat leaves were placed in a stomatal-opening solution (50 mM KNO_3, 10 mM MES, 50 μM $CaCl_2$, pH 6.15) for 3 h under a high-intensity light and then transferred to a solution containing 0, 10, and 20 μM ABA for 2 h. The epidermis was detached for stoma observation using an Axioskop 40 microscope (Carl Zeiss).

LCI and BiFC assays

LCI assays for the interactions between TaTIP41, TaTAP46, and the TaPP2As were performed in *N. benthamiana* leaves, as described previously (Liu et al., 2020). Full-length *TaTIP41* and *TaTAP46* CDSs were fused to the N-terminal and C-terminal regions of the *LUC* reporter gene, respectively (TaTIP41-nLUC and cLUC-TaTAP46). Similarly, full-length *TaPP2A* CDSs were used to generate TaPP2As-nLUC and cLUC-TaPP2As constructs. All nLUC and cLUC derivative constructs were transformed into *A. tumefaciens* strain GV3101 and then co-infiltrated into *N. benthamiana* leaves. LUC activity was imaged and analyzed 48–72 h after infiltration using the NightSHADE LB 985 Plant Imaging System (Berthold Technologies, Germany).

For the BiFC assays, the *TaTIP41* CDS was cloned into the pCAMBIA1300-nYFP and pCAMBIA1300-cYFP vectors to generate the TaTIP41-nYFP and TaTIP41-cYFP constructs, respectively. Similarly, the *TaTAP46* CDS was used to generate the TaTAP46-cYFP construct, and the *TaPP2As* CDSs were used to generate TaPP2As-nYFP constructs. The *A. tumefaciens* strain GV3101 cells harboring the nYFP and cYFP derivative constructs were co-infiltrated into *N. benthamiana* leaves, and YFP fluorescence signals were observed 72 h after infiltration under an LSM880 confocal laser-scanning microscope (Carl Zeiss).

Co-IP assay

To explore the interaction between TaTIP41 and TaTAP46 *in vivo*, the full-length *TaTIP41* CDS was cloned into p1300-35S-GFP to generate the TaTIP41-GFP construct, and the full-length *TaTAP46* CDS was cloned into p1300-35S-Flag to generate the Flag-TaTAP46 construct. The Flag-TaTAP46 and TaTIP41-GFP or GFP control constructs were transformed into *A. tumefaciens* strain GV3101 and then co-infiltrated into *N. benthamiana* leaves, which were harvested 72 h after infiltration. A Co-IP assay was performed as described previously (Li et al., 2023). In brief, the total proteins were extracted using the lysis buffer comprising 50 mM Tris-HCl (pH 7.5), 150 mM NaCl, 10% glycerol, 1% NP-40, 1 mM DTT, and 1× protease inhibitor cocktail. Anti-GFP-conjugated magnetic agarose beads (MBL, Japan) were used for the immunoprecipitation, and anti-GFP and anti-Flag antibodies (1:4,000 dilutions; ABclonal, China) were used for immunoblotting analysis.

PP2A activity assay

Wheat seedling leaves (three-leaf stage) were harvested from WT and *TaTIP41* and *TaTAP46* transgenic plants, ground in liquid nitrogen, and homogenized in an ice-cold sample buffer (50 mM Tris-HCl, pH 7.5, 1 mM EGTA, 0.02% β-mercaptoethanol, and protease inhibitor cocktail), as previously described (Ahn et al., 2011). Cell debris was removed by filtration through Miracloth (Calbiochem, USA), followed by centrifugation at 20,000 *g* at 4°C for 1 h. The protein concentration in the supernatant was determined using a Bradford protein assay kit (Zomanbio, China). PP2A activity was measured using the Ser/Thr Phosphatase Assay System (Promega, USA) according to the manufacturer's instructions.

VIGS-induced *TaPP2A-2* silencing

The BSMV-VIGS method was used to silence *TaPP2A-2* (*TraesCS5D02G465400*), following the protocol described previously (Ma et al., 2022). A 173-bp sequence derived from the *TaPP2A-2* CDS (nucleotides 669–841) was cloned into the silencing vector (BSMV*::TaPP2A-2*). Wheat seedlings at the two-leaf stage were infected with BSMV*::TaPDS* (positive control), 1× FES buffer (control check), BSMV*::*γ_0 (negative control), and BSMV*::TaPP2A-2*, following the method described by Hein et al. (2005). After infection, the wheat seedlings were sprayed with nuclease-free water and wrapped with a plastic film for high humidity. The wheat seedlings were placed in a growth chamber at 25°C in the dark for 24 h, after which a 16-h light/8-h dark photoperiod was maintained. After severe photobleaching was observed in the positive control plants, the growth conditions were set to a 16-h light/8-h

dark photoperiod at a 300 μmol/m^2/s light intensity and temperatures of 20°C (day) and 15°C (night).

ACKNOWLEDGEMENTS

We are grateful to Dr. Ke Wang (Institute of Crop Sciences, CAAS) for his help with wheat transformation. This research was financially supported by the National Key Research and Development Program of China (2022YFF1003402), the National Natural Science Foundation of China (32172045), the National Animal and Plant Transgenic Project (2016ZX08009001), and the Natural Science Foundation of Ningxia Province (2022AAC02056).

CONFLICTS OF INTEREST

The authors declare that they have no conflict of interests.

AUTHORS CONTRIBUTIONS

T.L., X.Z, and J.M. designed the research; J.M., Y.G., H.L, M. Z., S.L., Y.Z., and W.Z. performed the experiments; T.L., J. M., C.H., J.H., and D.Z. analyzed the data; T.L. and J.M. wrote the article; T.L. and X.Z. supervised and revised the writing of the article. All authors read and approved this manuscript.

Edited by: Pengcheng Wang, Southern University of Science and Technology, China

Received May 9, 2022; **Accepted** Jun. 12, 2023; **Published** Jun. 13, 2023

REFERENCES

Ahn, C.S., Ahn, H.K., and Pai, H.S. (2015). Overexpression of the PP2A regulatory subunit Tap46 leads to enhanced plant growth through stimulation of the TOR signalling pathway. J. Exp. Bot. **66:** 827–840.

Ahn, C.S., Han, J.A., Lee, H.S., and Pai, H.S. (2011). The PP2A regulatory subunit Tap46, a component of the TOR signaling pathway, modulates growth and metabolism in plants. Plant Cell **23:** 1185–1209.

Bates, L.S., Waldren, R.P., and Teare, I.D. (1973). Rapid determination of free proline for water-stress studies. Plant Soil **39:** 205–207.

Cutler, S.R., Rodriguez, P.L., Finkelstein, R.R., and Abrams, S.R. (2010). Abscisic acid: Emergence of a core signaling network. Annu. Rev. Plant Biol. **61:** 651–679.

Czechowski, T., Stitt, M., Altmann, T., Udvardi, M.K., and Scheible, W.R. (2005). Genome-wide identification and testing of superior reference genes for transcript normalization in *Arabidopsis*. Plant Physiol. **139:** 5–17.

Dobrenel, T., Caldana, C., Hanson, J., Robaglia, C., Vincentz, M., Veit, B., and Meyer, C. (2016). TOR signaling and nutrient sensing. Annu. Rev. Plant Biol. **67:** 261–285.

Fu, L., Liu, Y., Qin, G., Wu, P., Zi, H., Xu, Z., Zhao, X., Wang, Y., Li, Y., Yang, S., et al. (2021). The TOR-EIN2 axis mediates nuclear signalling to modulate plant growth. Nature **591:** 288–292.

Gingras, A.C., Caballero, M., Zarske, M., Sanchez, A., Hazbun, T.R., Fields, S., Sonenberg, N., Hafen, E., Raught, B., and Aebersold, R. (2005). A novel, evolutionarily conserved protein phosphatase complex involved in cisplatin sensitivity. Mol. Cell. Proteomics **4:** 1725–1740.

Hein, I., Barciszewska-Pacak, M., Hrubikova, K., Williamson, S., Dinesen, M., Soenderby, I.E., Sundar, S., Jarmolowski, A., Shirasu, K., and Lacomme, C. (2005). Virus-induced gene silencing-based functional characterization of genes associated with powdery mildew resistance in barley. Plant Physiol. **138:** 2155–2164.

Hu, R., Zhu, Y., Shen, G., and Zhang, H. (2014). TAP46 plays a positive role in the ABSCISIC ACID INSENSITIVE5-regulated gene expression in *Arabidopsis*. Plant Physiol. **164:** 721–734.

Huber, A., Bodenmiller, B., Uotila, A., Stahl, M., Wanka, S., Gerrits, B., Aebersold, R., and Loewith, R. (2009). Characterization of the rapamycin-sensitive phosphoproteome reveals that Sch9 is a central coordinator of protein synthesis. Genes Dev. **23:** 1929–1943.

IWGSC (2018). Shifting the limits in wheat research and breeding using a fully annotated reference genome. Science **361:** eaar7191.

Jacinto, E., Guo, B., Arndt, K.T., Schmelzle, T., and Hall, M.N. (2001). TIP41 interacts with TAP42 and negatively regulates the TOR signaling pathway. Mol. Cell **8:** 1017–1026.

Janssens, V., and Goris, J. (2001). Protein phosphatase 2A: A highly regulated family of serine/threonine phosphatases implicated in cell growth and signalling. Biochem. J. **353:** 417–439.

Lan, Y., Chawade, A., Kuktaite, R., and Johansson, E. (2022). Climate change impact on wheat performance-effects on vigour, plant traits and yield from early and late drought stress in diverse lines. Int. J. Mol. Sci. **23:** 3333.

Li, H., Liu, H., Hao, C., Li, T., Liu, Y., Wang, X., Yang, Y., Zheng, J., and Zhang, X. (2023). The auxin response factor TaARF15-A1 negatively regulates senescence in common wheat (*Triticum aestivum* L.). Plant Physiol. **191:** 1254–1271.

Li, T., Wu, X.Y., Li, H., Song, J.H., and Liu, J.Y. (2016). A dual-function transcription factor, AtYY1, is a novel negative regulator of the *Arabidopsis* ABA response network. Mol. Plant **9:** 650–661.

Li, Y., Wang, Y., Tan, S., Li, Z., Yuan, Z., Glanc, M., Domjan, D., Wang, K., Xuan, W., Guo, Y., et al. (2019). Root growth adaptation is mediated by PYLs ABA receptor-PP2A protein phosphatase complex. Adv. Sci. **7:** 1901455.

Liu, H., Li, H., Hao, C., Wang, K., Wang, Y., Qin, L., An, D., Li, T., and Zhang, X. (2020). *TaDA1*, a conserved negative regulator of kernel size, has an additive effect with *TaGW2* in common wheat (*Triticum aestivum* L.). Plant Biotechnol. J. **18:** 1330–1342.

Liu, Y., and Xiong, Y. (2022). Plant TOR signaling network: Complexes, conservations and specificities. J. Integr. Plant Biol. **64:** 342–370.

Livak, K.J., and Schmittgen, T.D. (2001). Analysis of relative gene expression data using real-time quantitative PCR and the $2^{-\Delta\Delta CT}$ method. Methods **25:** 402–408.

Ma, J., Tang, X., Sun, B., Wei, J., Ma, L., Yuan, M., Zhang, D., Shao, Y., Li, C., Chen, K.M., et al. (2022). A NAC transcription factor, *TaNAC5D-2*, acts as a positive regulator of drought tolerance through regulating water loss in wheat (*Triticum aestivum* L.). Environ. Exp. Bot. **196:** 104805.

Mao, H., Jian, C., Cheng, X., Chen, B., Mei, F., Li, F., Zhang, Y., Li, S., Du, L., Li, T., et al. (2022b). The wheat ABA receptor gene *TaPYL1-1B* contributes to drought tolerance and grain yield by increasing water-use efficiency. Plant Biotechnol. J. **20:** 846–861.

Mao, H., Li, S., Chen, B., Jian, C., Mei, F., Zhang, Y., Li, F., Chen, N., Li, T., Du, L., et al. (2022a). Variation in cis-regulation of a NAC transcription factor contributes to drought tolerance in wheat. Mol. Plant **15:** 276–292.

Mei, F., Chen, B., Du, L., Li, S., Zhu, D., Chen, N., Zhang, Y., Li, F., Wang, Z., Cheng, X., et al. (2022). A gain-of-function allele of a DREB

transcription factor gene ameliorates drought tolerance in wheat. Plant Cell **34:** 4472–4494.

Munemasa, S., Hauser, F., Park, J., Waadt, R., Brandt, B., and Schroeder, J.I. (2015). Mechanisms of abscisic acid-mediated control of stomatal aperture. Curr. Opin. Plant Biol. **28:** 154–162.

Nakashima, K., and Yamaguchi-Shinozaki, K. (2013). ABA signaling in stress-response and seed development. Plant Cell Rep. **32:** 959–970.

Nakashima, A., Tanimura-Ito, K., Oshiro, N., Eguchi, S., Miyamoto, T., Momonami, A., and Kikkawa, U. (2013). A positive role of mammalian Tip41-like protein, TIPRL, in the amino-acid dependent mTORC1-signaling pathway through interaction with PP2A. FEBS Lett. **587:** 2924–2929.

Pernas, M., García-Casado, G., Rojo, E., Solano, R., and Sánchez-Serrano, J.J. (2007). A protein phosphatase 2A catalytic subunit is a negative regulator of abscisic acid signalling. Plant J. **51:** 763–778.

Punzo, P., Ruggiero, A., Grillo, S., and Batelli, G. (2018b). TIP41 network analysis and mutant phenotypes predict interactions between the TOR and ABA pathways. Plant Signal. Behav. **13:** e1537698.

Punzo, P., Ruggiero, A., Possenti, M., Nurcato, R., Costa, A., Morelli, G., Grillo, S., and Batelli, G. (2018a). The PP2A-interactor TIP41 modulates ABA responses in *Arabidopsis thaliana*. Plant J. **94:** 991–1009.

Smetana, J.H., and Zanchin, N.I. (2007). Interaction analysis of the heterotrimer formed by the phosphatase 2A catalytic subunit, alpha4 and the mammalian ortholog of yeast Tip41 (TIPRL). FEBS J. **274:** 5891–5904.

Waadt, R., Manalansan, B., Rauniyar, N., Munemasa, S., Booker, M.A., Brandt, B., Waadt, C., Nusinow, D.A., Kay, S.A., Kunz, H.H., et al. (2015). Identification of open stomata1-interacting proteins reveals interactions with sucrose non-fermenting1-related protein kinases2 and with type 2A protein phosphatases that function in abscisic acid responses. Plant Physiol. **169:** 760–779.

Wang, K., Liu, H., Du, L., and Ye, X. (2017). Generation of marker-free transgenic hexaploid wheat via an *Agrobacterium*-mediated co-transformation strategy in commercial Chinese wheat varieties. Plant Biotechnol. J. **15:** 614–623.

Wullschleger, S., Loewith, R., and Hall, M.N. (2006). TOR signaling in growth and metabolism. Cell **124:** 471–484.

Yang, W., Zhang, W., and Wang, X. (2017). Post-translational control of ABA signalling: The roles of protein phosphorylation and ubiquitination. Plant Biotechnol. J. **15:** 4–14.

Zhang, Y., Li, T., Geng, Y., Wang, Y., Liu, Y., Li, H., Hao, C., Wang, H., Shang, X., and Zhang, X. (2021). Identification and development of a KASP functional marker of *TaTAP46-5A* associated with kernel weight in wheat (*Triticum aestivum*). Plant Breed **140:** 585–594.

Zhang, Y., Wang, J., Li, Y., Zhang, Z., Yang, L., Wang, M., Zhang, Y., Zhang, J., Li, C., Li, L., et al. (2023). Wheat TaSnRK2.10 phosphorylates TaERD15 and TaENO1 and confers drought tolerance when overexpressed in rice. Plant Physiol. **191:** 1344–1364.

Zhang, Z., Zhu, J.Y., Roh, J., Marchive, C., Kim, S.K., Meyer, C., Sun, Y., Wang, W., and Wang, Z.Y. (2016). TOR signaling promotes accumulation of BZR1 to balance growth with carbon availability in *Arabidopsis*. Curr. Biol. **26:** 1–7.

Zheng, Y., Jia, A., Ning, T., Xu, J., Li, Z., and Jiang, G. (2008). Potassium nitrate application alleviates sodium chloride stress in winter wheat cultivars differing in salt tolerance. J. Plant Physiol. **165:** 1455–1465.

SUPPORTING INFORMATION

Additional Supporting Information may be found online in the supporting information tab for this article: http://onlinelibrary.wiley.com/doi/10.1111/jipb.13542/suppinfo

Figure S1. Analysis of the phylogenetic tree and conserved domains of the TaTIP41 homoeologs

Figure S2. Subcellular localization of the TaTIP41 homoeologs in onion epidermal cells

Figure S3. Sequence alignment of the *TaTIP41* homoeologs and detection of *TaTIP41* expression in transgenic wheat lines

Figure S4. qRT-PCR analysis of *TaTAP46* expression under the PEG (A) and ABA (B) treatments

Figure S5. Sequence alignment of the *TaTAP46* homoeologs and detection of *TaTAP46* expression in transgenic wheat lines

Figure S6. TaTIP41 and TaTAP46 physically interact with TaPP2A-1 and TaPP2A-3

Figure S7. Silencing *TaPP2A-2* using a virus-induced gene silencing (VIGS) system improves drought tolerance in wheat